HHS Public Access

Author manuscript

Nat Med. Author manuscript; available in PMC 2016 October 25.

Published in final edited form as:

Nat Med. 2016 June ; 22(6): 641–648. doi:10.1038/nm.4084.

发作间期和记忆损伤

Interictal epileptiform discharges induce hippocampal-cortical coupling in temporal lobe epilepsy

Jennifer N. Gelinas[1], **Dion Khodagholy**[1], **Thomas Thesen**[2], **Orrin Devinsky**[2], and **György Buzsáki**[1,3,*]

[1]The Neuroscience Institute, New York University, School of Medicine, New York, NY, USA

[2]Department of Neurology, Comprehensive Epilepsy Center, New York University, School of Medicine, New York, NY, USA

[3]Center for Neural Science, New York University, School of Medicine, New York, NY, USA

Abstract

Interactions between the hippocampus and cortex are critical for memory. Interictal epileptiform discharges (IEDs) identify epileptic brain regions and can impair memory, but how they interact with physiological patterns of network activity is mostly undefined. We show in a rat model of temporal lobe epilepsy that spontaneous hippocampal IEDs correlate with impaired memory consolidation and are precisely coordinated with spindle oscillations in the prefrontal cortex during NREM sleep. This coordination surpasses the normal physiological ripple-spindle coupling and is accompanied by decreased ripple occurrence. IEDs also induce spindles during REM sleep and wakefulness, behavioral states that do not naturally express these oscillations, by generating a cortical 'DOWN' state. We confirm a similar correlation of temporofrontal IEDs with spindles over anatomically restricted cortical regions in a pilot clinical examination of four subjects with focal epilepsy. These findings imply that IEDs may impair memory via misappropriation of physiological mechanisms for hippocampal-cortical coupling, suggesting a target to treat memory impairment in epilepsy.

Introduction

Impairment of cognitive function, especially memory, is a common and disabling problem in individuals with temporal lobe epilepsy[1]. Clinical and experimental evidence demonstrate that pathological network activity occurring between seizures, the most prominent of which is interictal epileptiform discharges (IEDs), contribute to this dysfunction[2–8]. The specific cognitive consequences of IEDs are entangled with numerous pathological phenomena and

Correspondence should be addressed to G.B. gyorgy.buzsaki@nyumc.org.

Competing Financial Interests

The authors declare no competing financial interests.

Author contributions

J.N.G. and G.B. conceived the project. J.N.G. and D.K. did the rodent *in vivo* experiments. J.N.G. and D.K. analyzed rat and human neural data. T.T. and O.D. supervised the human epilepsy recordings and IRB. J.N.G., D.K., and G.B. wrote the paper with input from the other authors.

medication effects in these individuals. IEDs have been implicated in the development of cognitive deficits[7] and various aspects of memory[8–10]. Yet, how hippocampal IEDs communicate with the neocortex and affect computation in target structures remains unexplored.

Effective hippocampal-cortical communication is required for efficient memory function[11–13]. Three patterns of network activity and their physiological coupling are critical for memory consolidation: hippocampal ripples, neocortical slow oscillations, and neocortical sleep spindles[11]. Hippocampal ripples are brief, high-frequency (100–200 Hz) oscillations that coordinate and replay sequences of ordered neural firing related to experience[14,15]. Selective elimination of ripples severely impairs memory performance in rodents,[16,17] establishing their causal role in memory. Sleep spindles of non-rapid eye movement sleep (NREM) are lower frequency (9–16 Hz) oscillations generated within thalamocortical networks[18] that are also associated with sequential replay of neural firing[19]. During NREM sleep, ripples temporally correlate with sleep spindles via the slow oscillation in the neocortex.[20–23]

The medial prefrontal cortex (mPFC) is a key structure in hippocampal-dependent memory processes[24–26] that receives direct projections from the hippocampus via a pathway with bidirectional synaptic plasticity[27–30]. Co-activation of these structures, via temporal coupling of hippocampal ripples, neocortical slow oscillations, and spindles, is hypothesized to be essential for the consolidation of memory[31].

Given the precise synchronization of oscillations and neural firing between the hippocampus and mPFC during NREM sleep[31], introducing abnormal signals into this network could impair its function. Like physiological ripples, IEDs are enhanced in NREM sleep relative to wakefulness and REM (rapid eye movement) sleep[32], with specific facilitating effects attributed to the slow oscillation and/or epochs of spindling activity[33–35]. We hypothesized that hippocampal IEDs compete with physiological ripples and disrupt communication between hippocampus and mPFC, thereby impairing memory consolidation. To test this hypothesis, we used a kindling model of epilepsy to analyze the effects of hippocampal IEDs on spatial navigation memory and coordination of hippocampal and mPFC oscillations in the freely behaving rat. We demonstrate that hippocampal IEDs reliably induce spindles in the mPFC, and that IED frequency and coupling with mPFC spindles are both correlated with the degree of memory impairment. This pathological hippocampal-cortical coupling is more robust than physiological ripple-spindle coupling, and is mediated by the consistent initiation of a cortical ‘DOWN’ state that occurs regardless of behavioral state. We found similar IED-spindle coordination in subjects with epilepsy, providing a possible mechanism by which IEDs disrupt physiological memory networks.

Results

Evolution of hippocampal-cortical coupling in a rodent kindling model of epilepsy

We performed daily neurophysiological recordings in male and female adult Long-Evans rats implanted with intracranial depth electrodes in the hippocampus and mPFC over the course of hippocampal commissure kindling. Induction of repeated, electrically-induced

seizures (‘kindling’) is an established model of epilepsy that recapitulates numerous features of temporal lobe epilepsy, including chronic hyperexcitability of temporal lobe neurons, seizure semiology, associated comorbidities, and responsiveness to pharmacotherapy[36]. Kindling resulted in behavioral limbic seizures that became generalized over three weeks, with similar progression through Racine stages across animals (line plot; Fig. 1a). Rats also developed spontaneous hippocampal IEDs after a minimum of five days of kindling (Supplementary Fig. 1), with greater IED frequency in NREM sleep than REM sleep and waking (bar graph; Fig. 1a).

Since hippocampal-cortical coupling occurs during NREM sleep and IEDs are more frequent during this state, we identified characteristic NREM oscillations in the local field potential (LFP) of hippocampus and neocortex. Hippocampal ripples were detected in the pyramidal cell layer of the CA1 (cornu Ammonis 1) region[37], and spindles were detected in the deep layers of the mPFC. In agreement with previous research[22,23], we found that hippocampal ripples tend to precede mPFC spindles (Fig. 1b). Notably, IEDs in CA1 established strong temporal coupling with mPFC spindles (Fig. 1c).

Spindle occurrence in the mPFC remained relatively constant over the 18 d course of kindling, whereas hippocampal ripples decreased significantly ($P = 5 \times 10^{-9}$) in all animals over this same period. An increase in IED occurrence paralleled the timeline of decreased ripple occurrence, although the incidence was lower than that of ripples and did not fully compensate the ripple decrease (Fig. 1d). Kindling also modified characteristics of ripple oscillations, with a shift toward inclusion of both lower and higher frequency components (Supplementary Fig. 2).

Hippocampal IEDs impair memory

To determine whether these kindling-associated changes in the hippocampus-mPFC network have functional implications, we assessed performance of rats on the cheeseboard maze (Supplementary Video 1). This task requires reward-based planning that involves prefrontal connections[38] for which ripple-related replay of neuronal activity in the post-training consolidation period is essential for recall of learned reward configuration[39].

Over the course of 35 trials in each training session, rats accurately and consistently navigated to the location of three hidden rewards before returning to the starting box. Memory was assessed in a five trial test session performed the following day in the same spatial configuration as the previous day’s training session, followed by learning a new configuration. Because the reward locations were changed in each session, the rats were required to encode, consolidate, and subsequently retrieve a different memory for each session.

Each rat ($n = 6$) was tested across four phases: baseline, kindling, recovery, and artificial IEDs (Fig. 2a). These phases were aimed at disentangling the effects of seizures and interictal activity on behavioral performance. In the baseline phase, all rats learned the schema (Fig. 2b, left), and executed high levels of reward retrieval after an overnight consolidation period (Fig. 2b, right). Rats were then kindled, using an alternate day protocol to minimize the effect of seizures on behavioral performance (Fig. 2a). Task performance

decreased over the course of kindling in all rats, despite intact learning during the training session (Fig. 2c). This memory deficit was paralleled by increased IED and decreased ripple occurrence (Supplementary Fig. 3). To investigate potential long-lasting effects of seizures, we continued behavioral training and testing after kindling was completed. Performance improved across animals in this 'recovery' phase (Fig. 2d), along with increased ripple occurrence, low residual IED rate, and no seizures. Subsequently, to simulate the effect of IEDs without inducing further seizure activity, we induced artificial IEDs (a-IED) by delivering single electric pulses to the hippocampal commissure[40]. During this a-IED phase, performance again decreased in all animals (Fig. 2d). Memory performance in the kindled and a-IED phases was significantly lower than during the baseline and recovery phases ($P = 9.8 \times 10^{-4}$).

To specifically assess the impact of IEDs, we performed multivariate correlation of IED rate, IED-spindle coupling rate, ripple rate, and cumulative number of seizures with memory performance during the behavioral protocol (Fig. 2e). As expected, ripple rate was positively correlated with performance[39]. IED rate and IED-spindle coupling rate were strongly negatively correlated with performance, while cumulative seizure number yielded a more variable negative correlation. Together, these results demonstrate that IEDs impair cognition and that IEDs during the consolidation period adversely affect memory.

Hippocampal IEDs induce mPFC spindles

Since hippocampal IED-mPFC spindle coupling has a strong negative correlation with memory performance, we next aimed to quantify and characterize this interaction. During NREM sleep, hippocampal IEDs and mPFC spindles at their peak occurrence times were correlated within a narrow time window (average time offset from IED to spindle start = 410 ± 31 ms, across all animals; Supplementary Fig. 4), with IEDs consistently preceding the spindle oscillations. This temporal relationship was similar to the ripple-spindle timing, but much larger in magnitude and less variable across events (Fig. 3a). Variability was quantified across trials of IED occurrence using a Fano factor, with IEDs inducing a significantly greater decrease compared to ripples (Supplementary Fig. 5a–b; $P = 0.004$). Correspondingly, spindles followed IEDs at a significantly higher probability than ripples (Supplementary Fig. 5c; $P = 2 \times 10^{-4}$). The strong IED-spindle coupling was also reflected in the substantial increase in trigger-averaged spindle-band power after IEDs versus the moderate increase in spindle-band power after ripples (Fig. 3b). This power difference was quantified by comparing the mean change in mPFC power spectrum at spindle band before and after an IED or a ripple (Supplementary Fig. 5e; $P = 3 \times 10^{-5}$). The interval between ripple and spindle occurrence decreased in the kindled compared to unkindled state, though ripple-spindle coupling strength was similar (Supplementary Fig. 5d–f). These data suggest that hippocampal IEDs and ripples induce similar patterns of mPFC activity in NREM sleep, but IEDs are more potent.

We examined whether the IED-evoked mPFC spindles exhibited different oscillation characteristics than physiological spindles in normal rats, or spontaneous spindles in kindled rats. The average filtered spindle waveform was indistinguishable between the three conditions (Fig. 3c), and small differences in the duration and peak frequency of the

oscillations were not physiologically relevant (Fig. 3d–e). Thus, the fundamental temporal and morphological characteristics of IED-evoked spindles are the same as physiological spindles. Further, mPFC neurons that displayed significant phase synchrony to spindle oscillations maintained similar phase preference regardless of whether the spindle oscillation was spontaneous or IED-evoked (Fig. 3f).

Hippocampal IEDs evoke spindle oscillations across behavioral states

Physiological spindles are restricted to NREM sleep. Because IEDs occurred during all brain states, albeit at lower rates, we studied IED effects on mPFC during REM sleep and waking. Unexpectedly, hippocampal IEDs in REM and waking also induced spindle-like oscillations in the mPFC (Fig. 4a). To characterize these spindle-like oscillations, we normalized mPFC spectrograms using a baseline spectrum from each state, and calculated a trigger-averaged spectrogram based on occurrence of hippocampal IEDs. Hippocampal IEDs induced strong, precisely timed increases in the mPFC spindle band power regardless of behavioral state. Comparison of the mPFC power spectrum before and after IED occurrence confirmed marked increases in the spindle band during each state (Fig. 4b). Mean spindle-band power increased more in REM and waking states compared to NREM, largely due to the absence of spontaneous spindle activity in REM and waking states in the intact brain. The probability of spindle-like oscillations in the first second following an IED was significantly higher during REM than NREM (Fig. 4c; $P = 0.03$).

We next compared the characteristics of the spindle-like oscillations generated across behavioral states. The median duration of spindles was shorter in NREM relative to REM, with waking oscillations having intermediate values; however inter-animal variability was evident (Fig. 4d inset). The median peak frequency of spindle-like oscillations was significantly lower in REM than waking, a trend that was seen across animals, but the absolute difference was physiologically negligible (Fig. 4e; NREM = 13.3 Hz, REM = 12.6 Hz, Wake = 13.4 Hz; $P = 0.01$). These data suggest that hippocampal IEDs elicit similar cortical spindle responses in all brain states, with subtle differences in the oscillation features that vary in magnitude across animals.

Hippocampal IEDs evoke mPFC spindles via induction of a cortical ‘DOWN’ state

We examined mPFC LFP and spiking activity during the time window between hippocampal IED and mPFC spindle to elucidate the mechanisms of this interaction. Averaging deep layer mPFC LFP traces revealed a prominent positive delta wave within 400 ms after IED occurrence in all behavioral states (Fig. 5a–b). The spontaneous occurrence of delta waves during NREM elevated the baseline delta power above that in REM and waking as expected, but did not change the maximal delta power after IED occurrence. Hippocampal IED occurrence was associated with a consistent pattern of delta phase changes, as determined by deriving the continuous phase in this frequency band (2–5 Hz), and this pattern was similar in all states (Fig. 5c).

Deep layer positive cortical delta waves are characteristic of cortical ‘DOWN’ states, which are associated with neuronal hyperpolarization and decreased spiking during NREM sleep and anesthesia[41,42]. We constructed peristimulus time histograms from the average spiking

of clustered putative mPFC pyramidal cells and interneurons, with the hippocampal IEDs as stimuli. In all states and for both cell types, hippocampal IEDs induced a marked decrease in neuronal firing within 200 ms, consistent with the LFP delta wave, followed by an increased discharge of the putative interneurons (Fig. 5d). These results support the hypothesis that the synchronous hippocampal output generated by an IED can reset the mPFC slow oscillation phase, forcing a cortical 'DOWN' state characterized by an LFP delta wave and decreased neuronal firing. Recovery from this 'DOWN' state induces thalamocortical spindles[18]. Consistent with this notion, IEDs produce more profound changes in mPFC neural firing rates and gamma frequency (20–50 Hz) power than ripples (Supplementary Fig. 6).

We tested the hypothesis that synchronous hippocampal output can trigger the mPFC response by inducing a-IEDs[40]. In unkindled naïve rats, these a-IEDs consistently induced mPFC spindles only during NREM at high current intensity. In contrast, when similarly efficacious a-IEDs were applied in kindled rats increased spindle-band power was observed during NREM, and spindles were also generated in REM and waking (Supplementary Fig. 7). Thus, network changes associated with kindling modify mPFC circuits; one manifestation is facilitated expression of mPFC spindling in response to synchronous hippocampal output.

Temporofrontal lobe IEDs trigger cortical spindles in subjects with epilepsy

Although the kindling model mimics many features of temporal lobe epilepsy[36], not all pathological observations in kindled rats translate to humans. We analyzed sleep recordings from subjects with epilepsy implanted with subdural grid and strip, and depth electrodes for electrocorticography (ECoG) during surgical evaluation to assess possible temporal coupling between IEDs and cortical spindles. For each subject, an electrode with maximal IED amplitude was selected for IED detection. In three subjects, the IED electrode was located in the mesial temporal lobe structures, and in the fourth subject it was located in the frontal lobe (Supplementary Table 1). Despite variability in the number and location of electrodes exhibiting IEDs across subjects, in each case the detected IEDs were associated with sleep spindles on a restricted region of the cortical surface. Further, electrodes with high IED-spindle correlation did not exhibit IEDs, indicating that spindle generation occurred remotely and was synaptically driven.

The IED-spindle correlation in humans was demonstrated by three methods: (i) detection of oscillations in the cortical LFP fulfilling criteria for spindles after IED occurrence (Fig. 6a); (ii) spindle-band power increase after IED occurrence (Fig. 6b); (iii) significant cross-correlation between IEDs and spindles. A correlation value was derived for each electrode based on the significance of its IED-spindle cross-correlation, and these values were plotted as a heat map across the pial surface to localize the correlated brain regions (Fig. 6c). The location of correlated brain regions remained consistent across different days of recording in each subject. In all subjects, IEDs coupled with spindles in the superior, middle, and inferior frontal gyri (Supplementary Table 1). Although the frontal lobe contained a substantial percentage of correlation in all subjects, the anatomical distribution of correlation differed between subjects (Supplementary Table 2). Similar to our observations in kindled rats, in subjects with epilepsy, IEDs were associated with a subsequent increase in delta power and

resetting of the delta phase in cortical electrodes that exhibited high IED-spindle correlation (Fig. 6d).

Overall, the coupling of IEDs with spindles via a cortical 'DOWN' state appears to be a common manifestation of a temporofrontal epileptic network in rodents and humans.

Discussion

We demonstrate that spontaneous hippocampal IEDs establish strong, precisely timed coupling between the hippocampus and mPFC by consistently interrupting ongoing network activity with an induced cortical 'DOWN' state and spindle oscillation in sleeping and waking subjects. IED-spindle interactions represent a generalizable feature of temporofrontal epileptic networks in rodents and humans. Further, hippocampal IEDs and their downstream coupling to spindles are correlated with impairment of spatial memory consolidation in rats. This pathological hippocampal-cortical coupling may impair cognition in individuals with temporal lobe epilepsy.

We found that kindled rats had impaired memory consolidation on a hippocampus-dependent reward-based planning task. The experimental design was tailored to assay the effects of IEDs on memory performance. We conclude that IEDs contributed to the consolidation deficit because: i) during kindling, memory for spatial information acquired the previous day was dramatically reduced, even though learning and recall were carried out ~24 hours after any seizure activity; ii) post-kindling and without seizures, performance recovered in parallel with decreased incidence of IEDs, refuting a permanent residual effect of seizures; iii) induction of a-IEDs during the consolidation period, without any seizure activity, reinstated a memory deficit; iv) memory performance errors correlated most strongly with IED frequency and IED-spindle coupling. These results extend previous findings that IEDs occurring during waking behavior can affect sensory processing[43], and maintenance[10] and retrieval[9] of a short-term memory task.

Although previous experiments have reported correlations between IEDs and cognitive effects[6,7,44], their role in memory consolidation has not been previously established. Animal models of temporal lobe epilepsy exhibit changes in hippocampal physiology, including lower coherence of place cells despite intact cell sequence reactivation[45], altered phase precession[46], and deficits in theta oscillations[47]. Our focus on hippocampal-cortical interactions revealed that IEDs provide a means by which such pathological activity can be communicated to downstream brain regions across behavioral states. Because hippocampal ripple-cortical spindle coupling is implicated in memory consolidation[11], it is reasonable to hypothesize that IED-spindle coupling disrupts this process. This notion is supported by the significant correlation of IED-spindle coupling with poor long-term memory performance in our rats. However, causes of memory impairment in brain disorders are likely multifactorial, and determining the specific contribution of hippocampal-prefrontal coupling will require temporally-restricted manipulation of the neural network.

Our results suggest that IEDs interfere with both local hippocampal networks and synaptically connected cortical networks. In the hippocampus, ripples in the pyramidal layer

of area CA1 are triggered by synchronous bursts in area CA3, and these high frequency excitatory oscillations sequence neural firing,[48] allowing for efficient transfer of hippocampal information to the neocortex for memory formation[14,15]. In contrast, IEDs synchronize neural firing over a short temporal window (< 10 ms[49]), likely emerge from pathologically interacting neuronal clusters,[50] and interfere with physiological sequencing of neural firing. Although ripples and IEDs compete for the same anatomical substrates[14,51,52], they fundamentally differ in their spike pattern and content. These properties may explain the observed inverse relationship between ripple and IED occurrence during kindling.

Furthermore, we observed that IEDs exerted synaptically-driven effects on the mPFC, in support of previous observations that kindling can affect cortical circuits[53,54]. IEDs induced strong, synchronized patterns of mPFC neural firing associated with expression of delta waves and spindles, regardless of brain state. Thus, IEDs facilitate expression of cortical oscillations in brain states that do not naturally exhibit these oscillations, like REM and waking. This pathological coupling may be of diagnostic value because spindles can be visualized in electrocencephalogram (EEG) recordings. Therefore, the appearance of spindles in the cortical EEG during waking or REM could suggest IEDs in mesial temporal areas, the occurrence of which is difficult to detect non-invasively.

Hippocampal IEDs are most frequent during NREM sleep[32,51] and their occurrence correlates with the slow oscillation and/or epochs of increased spindle band power[34,35,55]. Similarly, IEDs generated by focal application of penicillin in the hippocampus of urethane-anesthetized rats correlate with the phase of local slow oscillations[33]. Such correlations indicate that periods of high synchronization favor IED occurrence. By contrast, our findings in rats and humans demonstrate that IEDs can reset the phase of slow oscillations and induce spindles.

In the intact brain, focal cortical electrical or magnetic stimulation during NREM sleep can induce a delta wave, often followed by a spindle[56,57], similar to the physiological K-complexes of slow oscillations that induce thalamocortical spindles[18]. Thus, the simplest interpretation of our findings is that synchronous hippocampal output during IEDs mimics the ‘stimulus’ that evokes a cortical ‘DOWN’ state which is followed by a spindle; the stronger the hippocampal output, the higher the probability of spindle induction. Hippocampal IEDs likely mobilize an existing physiological process in neocortex via interaction with thalamocortical networks mediating sleep oscillations. The close resemblance of IED-induced spindles in kindled rats to spontaneously occurring spindles in normal rats supports this notion.

All of our human subjects with epilepsy exhibited temporal coupling between IEDs and spindles similar to rats, and the frontal lobe consistently demonstrated preferential coupling. The precise localization and strength of IED-spindle coupling varied across subjects, and our correlation measures were limited to regions where electrodes were placed for clinical purposes. This variability may result from the heterogeneous nature of our population in regards to location and number of seizure foci, and anatomical distribution of interictal activity across limbic and cortical structures. Further investigation in subjects with varied seizure foci and other variables can clarify whether IED-spindle coupling is characteristic of

temporofrontal networks or a more general effect. The IED-induced cortical 'DOWN' state and coupled spindle activity supports observations showing alterations in the default mode network, including mPFC, during epileptic discharges[58].

Long-term memory requires a prolonged consolidation period, believe to be mediated by three prominent network patterns: hippocampal ripples, neocortical slow oscillations and thalamocortical sleep spindles[11]. Our results show that in the epileptic hippocampus, the incidence of ripples is decreased, while IEDs are frequent. Thus, the coordinated spiking organized by ripples needed for memory consolidation is replaced by IEDs that may broadcast 'nonsense' information as highly synchronized population activity to the mPFC. The cortex responds to this potent stimulus by generating a 'DOWN' state and subsequent spindle, recruiting mPFC neurons into events that carry no learning-related information and thereby may compete with true informational events. All three hypothesized pillars of memory consolidation[59] are therefore misused in the epileptic brain. Because IED-evoked spindles occur at a well-defined latency after an IED, this time window presents an opportunity for closed-loop investigations and therapeutics[60].

Online Methods

Animal surgical procedure

All animal experiments were approved by the Institutional Animal Care and Use Committee at New York University Langone Medical Center (NYULMC). Thirteen male and female Long Evans rats (200–350 g, 8–15 wks of age) were used for intracranial implantation. Sample size was estimated based on anticipated inter-animal neurophysiological variability, effect size of kindling on behavioral performance in previous studies, and low expected animal attrition. No rats were excluded from analysis. As each animal was tracked from baseline to kindled state, no randomization or blinding was utilized. Rats were kept on a regular 12h–12h light dark cycle and housed in pairs prior to implantation, but separated afterward. No prior experimentation had been performed on these rats. The animals were initially anaesthetized with 2% isoflurane and maintained under anesthesia with 0.75–1% isoflurane during the surgery. Silicon probes or tetrodes were implanted into right hippocampus (–3.5 AP, 3.0 ML) and right mPFC (+3.5 AP, 0.5–1.5 ML). Two tungsten wires with 50 μm diameter and 500 μm dorsoventral tip separation were attached together and implanted into the hippocampal commissure (–0.5 AP, 0.8 ML, –4.2 DV) for commissural electrical stimulation. Screws in the skull, overlying cerebellum, served as ground electrodes. The craniotomies were covered by Gelfoam and sealed using a 10:1 mixture of paraffin and mineral oil. Rats recovered for 4–5 days prior to initiation of experimentation. The hippocampal probe was then lowered to span layers of dorsal CA1 based on observation of key LFP features (e.g. ripples in the pyramidal cell layer). The mPFC tetrodes or probes were lowered to a depth of –3.5 DV, and correct placement was verified by observation of an extracellular postsynaptic potential (ePSP) in the mPFC recording following a population spike in the hippocampus elicited by delivery of a single pulse (0.1 ms pulse width, 25–100 μA) to the hippocampal commissure.

Neurophysiology data acquisition and processing

Seven of thirteen rats were used exclusively for neurophysiological recordings. These recording sessions started at a fixed time each morning. During the recording sessions, rats were exposed to an enriched environment (large enclosure containing a wheel) for 20 min and then returned to their homecage for baseline sleep recording. A subset of animals underwent delivery of test pulses to the hippocampal commissure (a-IEDs). This stimulation consisted of 0.1 ms duration square pulses delivered once per minute for 20–30 min. Current was titrated in steps with at least 30 min of no stimulation separating each session of pulse delivery. Rats were then started on the kindling procedure. After exposure to the enriched environment, 1 hr of pre-kindling data was obtained. Kindling stimulation consisted of 2 s duration bipolar current pulses (60 Hz, 1 ms pulse width). Amount of current used was determined on the initial kindling day by titrating current in 25 μA increments starting at 25 μA (1 min separation interval between stimulations) until a hippocampal seizure greater than 10 s duration was generated. This current setting was used for the remainder of kindling. Kindling stimulation was delivered twice per day. 3–6 hr of post-kindling data was then collected. Rats that underwent a-IED induction in the pre-kindled state were then subjected to the same stimulation protocol in the kindled state, using a range of current intensities. Neurophysiological signals were amplified, digitized continuously at 20 kHz using a head-stage directly attached to the probe (RHD2000 Intan technology), and stored for off-line analysis with 16-bit format. Data were analyzed using MATLAB (MathWorks) and visualized using Neuroscope.

Behavioral protocol

Animals—Six of the thirteen implanted rats were used for behavioral experiments in addition to neurophysiological recordings. These animals were placed on a water deprivation schedule for 3–5 days prior to intracranial implantation for familiarization with obtaining water via a hand-held syringe administered by the experimenter. Rats were weighed daily during water deprivation to ensure that body weight did not decrease to < 85% of pre-deprivation measurements. After the post-operative recovery period, rats were placed back on the water deprivation schedule for further behavioral training. Once consistent performance was attained, rats were sequentially advanced through 4 phases of the behavioral protocol: i) baseline – 4–6 paired training/testing sessions; ii) kindling – 14–18 d of kindling stimulation alternated with paired training/testing sessions; iii) rest/retraining/recovery – 10 d of rest (water ad libitum and no behavioral sessions) followed by 5 d of retraining on the behavioral task without recording, and subsequently 3 paired training/testing sessions without stimulation; iv) artificial IEDs – 2–4 paired training/testing sessions where a-IEDs were induced between training and testing. One animal was unable to complete the full protocol due to failure of the hippocampal probe during the recovery phase.

Apparatus—Behavior was tested on a cheeseboard maze, consisting of a 1.5 m diameter open circular arena that was painted a uniform green and stood 70 cm above the floor. A total of 177 water wells (7 mm in diameter, 3 mm in depth) were drilled 8 cm apart in the maze surface, forming evenly distributed, parallel columns and rows. One wall of the

starting box (23 cm wide × 30 cm long × 48 cm high) functioned as a drawbridge that could be raised and lowered to control the rat's access to the maze (Supplementary Video 1).

General task training—Water-deprived rats were first familiarized with exploring the maze environment to obtain water. Initially, the rat was placed in the center of the maze and allowed to explore and retrieve multiple (~25) randomly placed hidden water rewards. Over the next 3 d, the number of available water rewards on the maze was gradually reduced, and a trial structure introduced such that the rat received a food reward (0.5–1 Froot Loop) after successful retrieval of all water rewards. The rat was then trained to return to the starting box to obtain its food reward. After 2–4 d of this repeated procedure, the rat would consistently explore the maze to obtain three hidden water rewards and then return to the starting box to obtain its food reward. To prevent use of odor-mediated searching, the maze was wiped with a towel soaked in 70% ethanol and rotated by random degrees relative to the starting box between all trials. This phase of general training ended when the rat could complete 35 trials/d, with efficient retrieval of three rewards after the first 5–10 learning trials.

Paired training/testing sessions—After acquiring the scheme of the task, rats were started on the behavioral protocol, consisting of paired training/testing sessions each spanning 2 d. On the first of the two days, the rats learned the location of three hidden water rewards placed in randomly selected water wells over the course of ~35 trials (25 trial session, then ~1 h homecage rest, then 10 trial session). On the second of the two days, the rat was given a 5 trial probe test with water rewards located in the same location as the first day to assess memory for the spatial configuration of the reward locations. This test structure was chosen for two main reasons: i) it takes advantage of the rat's natural foraging behavior (efficient return to remembered reward locations, followed by exploration of other areas if rewards are not found at remembered locations, or reward locations are not remembered); and ii) rats require > five trials to learn three new reward locations. The training for the next training/testing session was then initiated (> 4 h after the testing session) with three different water reward locations. Training and testing sessions were monitored by an overhead video camera (10 frames/s), and tracking of the rat's location was facilitated by blue and red LEDs attached to its cap.

Protocol phases—During all phases, rats had neurophysiological recording in their home cage between training sessions (~1 h), after the last training session (~2 h), and after testing (~2 h). In the baseline and recovery phases, no additional interventions were introduced. During the kindling phase, seizures were induced and recorded in the homecage. Rats were kindled using an alternate day protocol (one seizure on the first day, followed by 3–4 seizures every alternate day), such that behavioral training occurred on a day when *no seizure activity was induced*. Testing for this training session was performed the next day, and kindling stimulation was administered *after* the test session. In this way, behavioral training and testing occurred 24 h after seizure induction. Previous work has indicated that most seizure-induced changes in hippocampal physiology reverse within 24 h[61–63]. In this design, deficits seen on behavioral testing would therefore more likely reflect interictal (IEDs) rather than ictal processes. No neurophysiological recordings were performed in the rest and retraining phase. In the a-IEDs phase, repetitive stimulation was delivered to the

hippocampal commissure (0.5 Hz, 500 μs pulse width) for the duration of the neurophysiological recording session between and after training sessions. Current was titrated to generate a hippocampal population spike in each animal.

Behavioral analysis—Behavioral performance was assayed using the animal's position in the tracking data. Learning performance was assessed by repeated, successful retrieval of all three rewards in < 30 s in a given trial during the training session. Memory performance score was assessed in the test session by the number of rewards obtained in < 30 s.

Rat LFP and spiking data processing

Recordings were classified into wake, REM, and NREM epochs based on theta/delta ratio calculated from the power spectrogram in concert with a movement vector extracted from synchronized onboard accelerometer. Spindle detection was initiated by filtering a channel recorded from deep layers of mPFC between 10–20 Hz, rectifying, and normalizing the signal. Spindle events were identified when the envelope was at least two standard deviations (SD) above the baseline (for a minimum of 400 ms and a maximum of 3 s) and the peak envelope was at least 3 SD above the baseline. For ripple detection, the hippocampal LFP from the CA1 pyramidal layer was band-pass filtered in the ripple frequency range (100–250 Hz). The signal was then rectified and normalized. Ripple events were identified when the envelope was at least 3 SD above the baseline (for a minimum of 20 ms and a maximum of 100 ms) and the peak envelope was at least 6 SD above the baseline. IEDs were detected as follows: (i) band-pass filtering at 60–80 Hz and signal rectification; (ii) detection of events where the filtered envelope was > 3 times above baseline; (iii) elimination of events with unfiltered envelope was < 3 times above baseline. Filter frequency for IEDs was selected empirically, based on the strong power of the IEDs in this band combined with a lack of overlap with ripples or other large amplitude physiological events co-existing in this band. Because sharp transients (including IEDs) can produce oscillations after high frequency filtering that could be detected as ripples, all detected IEDs were cross-referenced with detected ripples, and any events detected as both an IED and ripple were classified as IED events only. Detected IEDs had waveforms consistent with characteristic IED events[51,52] (Supplementary Fig. 1a). All detections were visually inspected for accuracy for each recording session. Occurrence rates of all the above events were calculated based on the daily pre-kindling recording to prevent any influence of the transient post-ictal state induced by kindling.

Extracellular spikes were identified by amplitude thresholding after high-pass filtering (> 300 Hz). The first three normalized principal components of the spike waveforms were input into KlustaKwik clustering program to generate putative single units. The clustering classification was manually inspected and refined using Klusters. Units were classified as pyramidal cells or interneurons based on waveform symmetry and mean wideband spike width[64].

Histology

Rats were euthanized with sodium pentobarbital and perfused via the heart with 0.9% saline followed by 10% formalin. Whole brains were extracted and sectioned using a vibratome

(Leica) to create 70 μm coronal slices. Slices were mounted on gelatin-coated glass slides, stained using a modified hematoxylin-eosin staining protocol, and cover-slipped. A light transmission microscope (Zeiss) was used to visualize and photograph the slices. Tetrode or probe location was reconstructed from adjacent slices.

Subjects with epilepsy LFP data processing

Analysis of clinical subdural ECoG recordings was approved by the Institutional Review Board at New York University Langone Medical Center (NYULMC). Informed written consent was obtained from all subjects. Sleep ECoG recordings (three sessions per subject) were obtained from four male and female subjects implanted with subdural grid electrodes and depth electrodes as part of the work-up for epilepsy surgery. Sample size required (number of subjects and recording sessions) was extrapolated from results of animal studies. Subjects with multiple days of continuous high quality ECoG recordings that included temporal and frontal regions were pre-established to be eligible for the study. Subjects with diffuse cortical lesions were excluded. Four subjects meeting these criteria with readily available data were randomly selected for further analysis. As no experimental manipulation was performed, there was no blinding or randomization employed. Epochs of seizure activity were excluded from analysis. Crude determination of sleep epochs was performed by extraction of a motion vector from video files in concert with delta/gamma ratio from the power spectrogram. ECoG data was imported into Matlab and resampled from 512 to 1250 Hz for analysis. Spindle detection was performed on each channel as in the rat, although SD thresholds were increased to accommodate the noisier recording quality (3 SD start; 4 SD peak). Electrodes chosen for IED detection were clinically verified to contain IEDs, and demonstrated maximal amplitude among neighboring electrodes. IED detection was also performed as in the rat, with modifications: (i) band-pass filtering was performed at 25–80 Hz to account for the wider waveforms of IEDs observed; (ii) thresholds were adjusted to two times above baseline; (iii) IEDs occurring within 1 s of another IED were excluded to prevent over-correlation due to a run of IEDs. Detected IEDs had waveforms consistent with typical interictal spikes and/or sharp waves (Supplementary Fig. 1b). All detections were visually inspected for accuracy for each recording session. Localization of grid and depth electrodes was performed based on reconstruction of subject specific pial surfaces, co-registration of pre- and post-implant MRI images, a combination of manual and automatic localization of electrodes, and subsequent co-registration to a standard template brain[65]. The gyral location of electrodes was determined based on cortical parcellation using the Desikan-Killiany atlas[66].

Statistics

Statistical analysis was performed using a combination of freely available, online Matlab toolboxes (Freely Moving Animal Toolbox; http://fmatoolbox.sourceforge.net), and custom Matlab code. Spectrograms were generated using wavelet transformation (Gabor) and power spectrums were calculated as mean ± standard error of the mean (s.e.m.) over trials. The instantaneous LFP phase was extracted by Hilbert transform. Significant changes in event occurrence over time were tested using a non-parametric monotonic trend test (Man-Kendall tau with Sen's method). Significance of cross-correlograms was calculated using a modified convolution method[67]. IED or ripple times were taken as cross-correlogram reference. Units

were deemed to have phase-locking to spindle oscillations when $\alpha < 0.05$ and $\kappa > 0.1$ on Rayleigh is test of non-uniformity. Probability distributions were compared using two-sample Kolmogorov-Smirnov tests with correction for multiple comparisons. Differences between groups were calculated using non-parametric ranksum (Wilcoxon) or ANOVA (Kruskal-Wallis with Bonferroni correction) depending on the nature of the data analyzed. Correlations were calculated using a correlation coefficient matrix based on the covariance of input variables. Error bars represent s.e.m. Significance level was $P < 0.05$.

Supplementary Material

Refer to Web version on PubMed Central for supplementary material.

Acknowledgments

This work was supported by the National Institute of Health Grants (NS074015, MH54671, MH102840; G.B.), the National Science Foundation (G.B.), the Mathers Foundation (G.B.), and the James S. McDonnell Foundation (G.B.). J.N.G. is a fellow of the Pediatric Scientist Development Program, and this project was supported through the March of Dimes Foundation. D.K. is supported through the Simons Foundation (junior fellow). We thank A. Peyrache for fruitful discussion, J. Long for use of the cheeseboard maze and advice on behavioral protocol, and Z. Zhao for technical support. We thank K. Berry, A. Boomhaur and P. del Prato for providing access to the sleep ECoG epilepsy data. Thanks also to H.X. Wang for providing the MRI-based electrode localizations for this data.

References

1. Hermann BP, Seidenberg M, Dow C, et al. Cognitive prognosis in chronic temporal lobe epilepsy. Ann Neurol. 2006; 60(1):80–87. [PubMed: 16802302]
2. Ebus S, Arends J, Hendriksen J, et al. Cognitive effects of interictal epileptiform discharges in children. European journal of paediatric neurology : EJPN : official journal of the European Paediatric Neurology Society. 2012; 16(6):697–706. [PubMed: 22750349]
3. Lv Y, Wang Z, Cui L, Ma D, Meng H. Cognitive correlates of interictal epileptiform discharges in adult patients with epilepsy in China. Epilepsy Behav. 2013; 29(1):205–210. [PubMed: 23994830]
4. Binnie CD. Cognitive impairment during epileptiform discharges: is it ever justifiable to treat the EEG? The Lancet. Neurology. 2003; 2(12):725–730. [PubMed: 14636777]
5. Brinciotti M, Matricardi M, Paolella A, Porro G, Benedetti P. Neuropsychological correlates of subclinical paroxysmal EEG activity in children with epilepsy. 1: Qualitative features (generalized and focal abnormalities). Functional neurology. 1989; 4(3):235–239. [PubMed: 2792857]
6. Holmes GL, Lenck-Santini PP. Role of interictal epileptiform abnormalities in cognitive impairment. Epilepsy Behav. 2006; 8(3):504–515. [PubMed: 16540376]
7. Khan OI, Zhao Q, Miller F, Holmes GL. Interictal spikes in developing rats cause long-standing cognitive deficits. Neurobiol Dis. 2010; 39(3):362–371. [PubMed: 20452427]
8. Krauss GL, Summerfield M, Brandt J, Breiter S, Ruchkin D. Mesial temporal spikes interfere with working memory. Neurology. 1997; 49(4):975–980. [PubMed: 9339676]
9. Kleen JK, Scott RC, Holmes GL, Lenck-Santini PP. Hippocampal interictal spikes disrupt cognition in rats. Ann Neurol. 2010; 67(2):250–257. [PubMed: 20225290]
10. Kleen JK, Scott RC, Holmes GL, et al. Hippocampal interictal epileptiform activity disrupts cognition in humans. Neurology. 2013; 81(1):18–24. [PubMed: 23685931]
11. Diekelmann S, Born J. The memory function of sleep. Nature reviews. Neuroscience. 2010; 11(2): 114–126. [PubMed: 20046194]
12. Maviel T, Durkin TP, Menzaghi F, Bontempi B. Sites of neocortical reorganization critical for remote spatial memory. Science (New York, NY). 2004; 305(5680):96–99.
13. Remondes M, Schuman EM. Role for a cortical input to hippocampal area CA1 in the consolidation of a long-term memory. Nature. 2004; 431(7009):699–703. [PubMed: 15470431]

14. Buzsaki G. Two-stage model of memory trace formation: a role for "noisy" brain states. Neuroscience. 1989; 31(3):551–570. [PubMed: 2687720]
15. Wilson MA, McNaughton BL. Reactivation of hippocampal ensemble memories during sleep. Science (New York, NY). 1994; 265(5172):676–679.
16. Girardeau G, Benchenane K, Wiener SI, Buzsaki G, Zugaro MB. Selective suppression of hippocampal ripples impairs spatial memory. Nat Neurosci. 2009; 12(10):1222–1223. [PubMed: 19749750]
17. Jadhav SP, Kemere C, German PW, Frank LM. Awake hippocampal sharp-wave ripples support spatial memory. Science (New York, NY). 2012; 336(6087):1454–1458.
18. Steriade M, McCormick DA, Sejnowski TJ. Thalamocortical oscillations in the sleeping and aroused brain. Science (New York, NY). 1993; 262(5134):679–685.
19. Johnson LA, Euston DR, Tatsuno M, McNaughton BL. Stored-trace reactivation in rat prefrontal cortex is correlated with down-to-up state fluctuation density. J Neurosci. 2010; 30(7):2650–2661. [PubMed: 20164349]
20. Battaglia FP, Benchenane K, Sirota A, Pennartz CM, Wiener SI. The hippocampus: hub of brain network communication for memory. Trends in cognitive sciences. 2011; 15(7):310–318. [PubMed: 21696996]
21. Molle M, Yeshenko O, Marshall L, Sara SJ, Born J. Hippocampal sharp wave-ripples linked to slow oscillations in rat slow-wave sleep. J Neurophysiol. 2006; 96(1):62–70. [PubMed: 16611848]
22. Peyrache A, Battaglia FP, Destexhe A. Inhibition recruitment in prefrontal cortex during sleep spindles and gating of hippocampal inputs. Proceedings of the National Academy of Sciences of the United States of America. 2011; 108(41):17207–17212. [PubMed: 21949372]
23. Siapas AG, Wilson MA. Coordinated interactions between hippocampal ripples and cortical spindles during slow-wave sleep. Neuron. 1998; 21(5):1123–1128. [PubMed: 9856467]
24. Churchwell JC, Morris AM, Musso ND, Kesner RP. Prefrontal and hippocampal contributions to encoding and retrieval of spatial memory. Neurobiology of learning and memory. 2010; 93(3): 415–421. [PubMed: 20074655]
25. Gais S, Albouy G, Boly M, et al. Sleep transforms the cerebral trace of declarative memories. Proceedings of the National Academy of Sciences of the United States of America. 2007; 104(47): 18778–18783. [PubMed: 18000060]
26. Jones MW, Wilson MA. Theta rhythms coordinate hippocampal-prefrontal interactions in a spatial memory task. PLoS biology. 2005; 3(12):e402. [PubMed: 16279838]
27. Jay TM, Burette F, Laroche S. NMDA receptor-dependent long-term potentiation in the hippocampal afferent fibre system to the prefrontal cortex in the rat. Eur J Neurosci. 1995; 7(2): 247–250. [PubMed: 7757261]
28. Jay TM, Witter MP. Distribution of hippocampal CA1 and subicular efferents in the prefrontal cortex of the rat studied by means of anterograde transport of Phaseolus vulgaris-leucoagglutinin. The Journal of comparative neurology. 1991; 313(4):574–586. [PubMed: 1783682]
29. Takita M, Izaki Y, Jay TM, Kaneko H, Suzuki SS. Induction of stable long-term depression in vivo in the hippocampal-prefrontal cortex pathway. Eur J Neurosci. 1999; 11(11):4145–4148. [PubMed: 10583503]
30. Varela C, Kumar S, Yang JY, Wilson MA. Anatomical substrates for direct interactions between hippocampus, medial prefrontal cortex, and the thalamic nucleus reuniens. Brain structure & function. 2014; 219(3):911–929. [PubMed: 23571778]
31. Colgin LL. Oscillations and hippocampal-prefrontal synchrony. Curr Opin Neurobiol. 2011; 21(3): 467–474. [PubMed: 21571522]
32. Malow BA, Lin X, Kushwaha R, Aldrich MS. Interictal spiking increases with sleep depth in temporal lobe epilepsy. Epilepsia. 1998; 39(12):1309–1316. [PubMed: 9860066]
33. de Guzman PH, Nazer F, Dickson CT. Short-duration epileptic discharges show a distinct phase preference during ongoing hippocampal slow oscillations. J Neurophysiol. 2010; 104(4):2194–2202. [PubMed: 20719925]
34. Ferrillo F, Beelke M, De Carli F, et al. Sleep-EEG modulation of interictal epileptiform discharges in adult partial epilepsy: a spectral analysis study. Clin Neurophysiol. 2000; 111(5):916–923. [PubMed: 10802464]

35. Nobili L, Ferrillo F, Baglietto MG, et al. Relationship of sleep interictal epileptiform discharges to sigma activity (12–16 Hz) in benign epilepsy of childhood with rolandic spikes. Clin Neurophysiol. 1999; 110(1):39–46. [PubMed: 10348319]
36. Morimoto K, Fahnestock M, Racine RJ. Kindling and status epilepticus models of epilepsy: rewiring the brain. Prog Neurobiol. 2004; 73(1):1–60. [PubMed: 15193778]
37. Buzsaki G, Horvath Z, Urioste R, Hetke J, Wise K. High-frequency network oscillation in the hippocampus. Science (New York, NY). 1992; 256(5059):1025–1027.
38. Chersi F, Burgess N. The Cognitive Architecture of Spatial Navigation: Hippocampal and Striatal Contributions. Neuron. 2015; 88(1):64–77. [PubMed: 26447573]
39. Dupret D, O'Neill J, Pleydell-Bouverie B, Csicsvari J. The reorganization and reactivation of hippocampal maps predict spatial memory performance. Nat Neurosci. 2010; 13(8):995–1002. [PubMed: 20639874]
40. Shatskikh TN, Raghavendra M, Zhao Q, Cui Z, Holmes GL. Electrical induction of spikes in the hippocampus impairs recognition capacity and spatial memory in rats. Epilepsy Behav. 2006; 9(4): 549–556. [PubMed: 17027341]
41. Buzsaki G, Bickford RG, Ponomareff G, Thal LJ, Mandel R, Gage FH. Nucleus basalis and thalamic control of neocortical activity in the freely moving rat. J Neurosci. 1988; 8(11):4007–4026. [PubMed: 3183710]
42. Steriade M, Nunez A, Amzica F. Intracellular analysis of relations between the slow (< 1 Hz) neocortical oscillation and other sleep rhythms of the electroencephalogram. J Neurosci. 1993; 13(8):3266–3283. [PubMed: 8340807]
43. Shewmon DA, Erwin RJ. The effect of focal interictal spikes on perception and reaction time. I. General considerations. Electroencephalogr Clin Neurophysiol. 1988; 69(4):319–337. [PubMed: 2450731]
44. Holmes GL. EEG abnormalities as a biomarker for cognitive comorbidities in pharmacoresistant epilepsy. Epilepsia. 2013; 54(Suppl 2):60–62. [PubMed: 23646973]
45. Titiz AS, Mahoney JM, Testorf ME, Holmes GL, Scott RC. Cognitive impairment in temporal lobe epilepsy: role of online and offline processing of single cell information. Hippocampus. 2014; 24(9):1129–1145. [PubMed: 24799359]
46. Lenck-Santini PP, Holmes GL. Altered phase precession and compression of temporal sequences by place cells in epileptic rats. J Neurosci. 2008; 28(19):5053–5062. [PubMed: 18463258]
47. Marcelin B, Chauviere L, Becker A, Migliore M, Esclapez M, Bernard C. h channel-dependent deficit of theta oscillation resonance and phase shift in temporal lobe epilepsy. Neurobiol Dis. 2009; 33(3):436–447. [PubMed: 19135151]
48. Nadasdy Z, Hirase H, Czurko A, Csicsvari J, Buzsaki G. Replay and time compression of recurring spike sequences in the hippocampus. J Neurosci. 1999; 19(21):9497–9507. [PubMed: 10531452]
49. Bragin A, Engel J Jr, Wilson CL, Fried I, Mathern GW. Hippocampal and entorhinal cortex high-frequency oscillations (100--500 Hz) in human epileptic brain and in kainic acid--treated rats with chronic seizures. Epilepsia. 1999; 40(2):127–137. [PubMed: 9952257]
50. Bragin A, Wilson CL, Engel J Jr. Chronic epileptogenesis requires development of a network of pathologically interconnected neuron clusters: a hypothesis. Epilepsia. 2000; 41(Suppl 6):S144–152. [PubMed: 10999536]
51. Buzsaki G, Hsu M, Slamka C, Gage FH, Horvath Z. Emergence and propagation of interictal spikes in the subcortically denervated hippocampus. Hippocampus. 1991; 1(2):163–180. [PubMed: 1669291]
52. Wadman WJ, Da Silva FH, Leung LW. Two types of interictal transients of reversed polarity in rat hippocampus during kindling. Electroencephalogr Clin Neurophysiol. 1983; 55(3):314–319. [PubMed: 6186463]
53. Bernhardt BC, Worsley KJ, Kim H, Evans AC, Bernasconi A, Bernasconi N. Longitudinal and cross-sectional analysis of atrophy in pharmacoresistant temporal lobe epilepsy. Neurology. 2009; 72(20):1747–1754. [PubMed: 19246420]
54. Kleen JK, Wu EX, Holmes GL, Scott RC, Lenck-Santini PP. Enhanced oscillatory activity in the hippocampal-prefrontal network is related to short-term memory function after early-life seizures. J Neurosci. 2011; 31(43):15397–15406. [PubMed: 22031886]

55. Frauscher B, von Ellenrieder N, Ferrari-Marinho T, Avoli M, Dubeau F, Gotman J. Facilitation of epileptic activity during sleep is mediated by high amplitude slow waves. Brain. 2015; 138(Pt 6): 1629–1641. [PubMed: 25792528]

56. Massimini M, Ferrarelli F, Esser SK, et al. Triggering sleep slow waves by transcranial magnetic stimulation. Proceedings of the National Academy of Sciences of the United States of America. 2007; 104(20):8496–8501. [PubMed: 17483481]

57. Vyazovskiy VV, Faraguna U, Cirelli C, Tononi G. Triggering slow waves during NREM sleep in the rat by intracortical electrical stimulation: effects of sleep/wake history and background activity. J Neurophysiol. 2009; 101(4):1921–1931. [PubMed: 19164101]

58. Fahoum F, Zelmann R, Tyvaert L, Dubeau F, Gotman J. Epileptic discharges affect the default mode network--FMRI and intracerebral EEG evidence. PloS one. 2013; 8(6):e68038. [PubMed: 23840805]

59. Inostroza M, Born J. Sleep for preserving and transforming episodic memory. Annual review of neuroscience. 2013; 36:79–102.

60. Krook-Magnuson E, Gelinas JN, Soltesz I, Buzsaki G. Neuroelectronics and Biooptics: Closed-Loop Technologies in Neurological Disorders. JAMA neurology. 2015

61. Peele DB, Gilbert ME. Functional dissociation of acute and persistent cognitive deficits accompanying amygdala-kindled seizures. Behavioural brain research. 1992; 48(1):65–76. [PubMed: 1622555]

62. Liu X, Muller RU, Huang LT, et al. Seizure-induced changes in place cell physiology: relationship to spatial memory. J Neurosci. 2003; 23(37):11505–11515. [PubMed: 14684854]

63. Boukhezra O, Riviello P, Fu DD, et al. Effect of the postictal state on visual-spatial memory in immature rats. Epilepsy Res. 2003; 55(3):165–175. [PubMed: 12972171]

64. Stark E, Eichler R, Roux L, Fujisawa S, Rotstein HG, Buzsaki G. Inhibition-induced theta resonance in cortical circuits. Neuron. 2013; 80(5):1263–1276. [PubMed: 24314731]

65. Yang AI, Wang X, Doyle WK, et al. Localization of dense intracranial electrode arrays using magnetic resonance imaging. Neuroimage. 2012; 63(1):157–165. [PubMed: 22759995]

66. Desikan RS, Segonne F, Fischl B, et al. An automated labeling system for subdividing the human cerebral cortex on MRI scans into gyral based regions of interest. Neuroimage. 2006; 31(3):968–980. [PubMed: 16530430]

67. Stark E, Abeles M. Unbiased estimation of precise temporal correlations between spike trains. J Neurosci Methods. 2009; 179(1):90–100. [PubMed: 19167428]

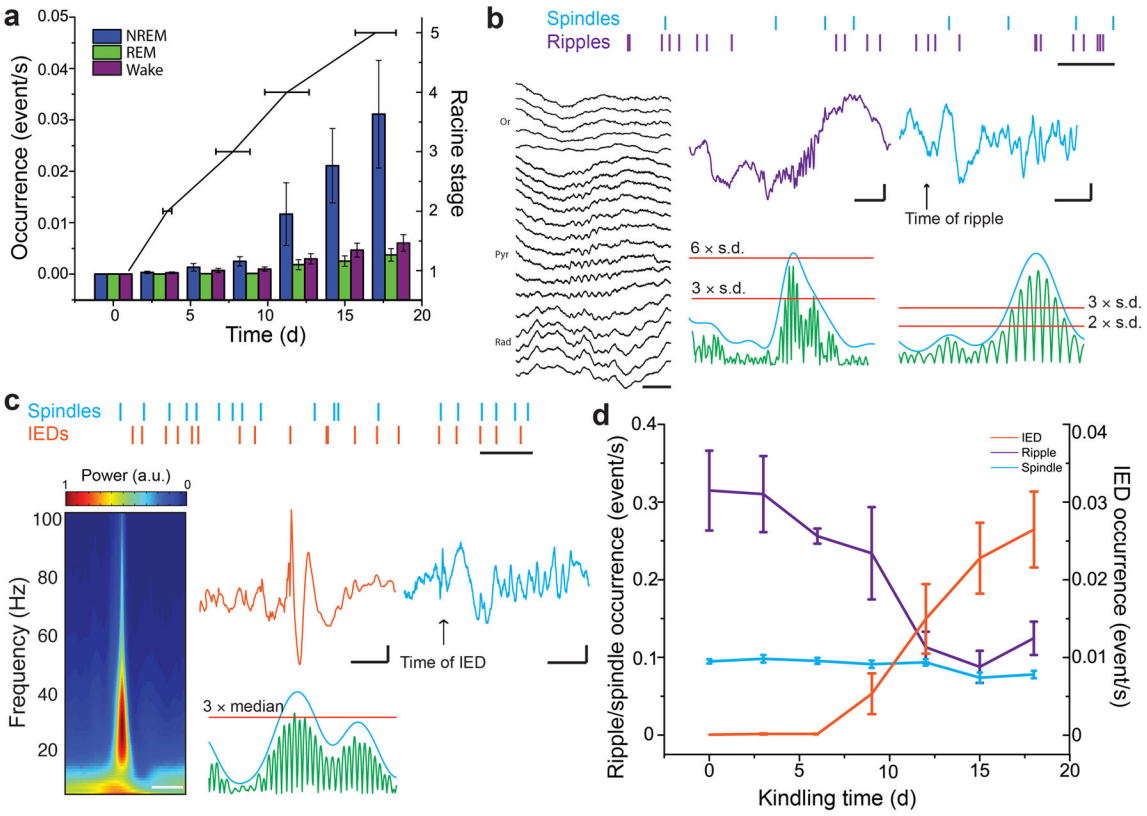

Figure 1.

Occurrence, detection, and coupling of hippocampal and mPFC oscillations during kindling. (**a**) Occurrence of IEDs in NREM, REM and Wake (bars) and increase in Racine stage (line) during kindling. Error bars = Mean ± s.e.m.; $n = 4$ rats. (**b**) Raster plot of mPFC spindles (blue) and hippocampal ripples (purple; scale bar = 10 s). Sample recorded ripple (black; Or = stratum oriens, Pyr = stratum pyramidale, Rad = stratum radiatum; scale bar = 30 ms). Raw LFP of detected ripple (purple; scale bar = 100 μV, 50 ms) with filtered (100–250 Hz), rectified version (bottom left; s.d. = standard deviation). Raw LFP of detected mPFC spindle associated with ripple (blue; scale bar = 100 μV, 500 ms) alongside filtered (10–20 Hz), rectified version (bottom right). (**c**) Raster plot of mPFC spindles (blue) and hippocampal IEDs (orange) after 14 d of kindling (scale bar = 10 s). Averaged spectrogram of hippocampal IED (scale bar = 500 ms). Raw LFP of detected IED (orange; scale bar = 200 μV, 100 ms) with filtered (60–80 Hz), rectified version. Detected mPFC spindle evoked by IED (blue; scale bar = 100 μV, 500 ms). (**d**) Occurrence of ripples, spindles, and IEDs in NREM sleep over 18 d of kindling. Error bars = Mean ± s.e.m.; $n = 4$ rats. Occurrence of spindles has a non-significant trend toward decrease over time (Mann Kendall tau (τ) = –0.16; $P = 0.065$; Z-test) whereas ripples decrease significantly ($\tau = -0.52$; $P = 5 \times 10^{-9}$) and IEDs increase ($\tau = 0.65$; $P = 5 \times 10^{-12}$).

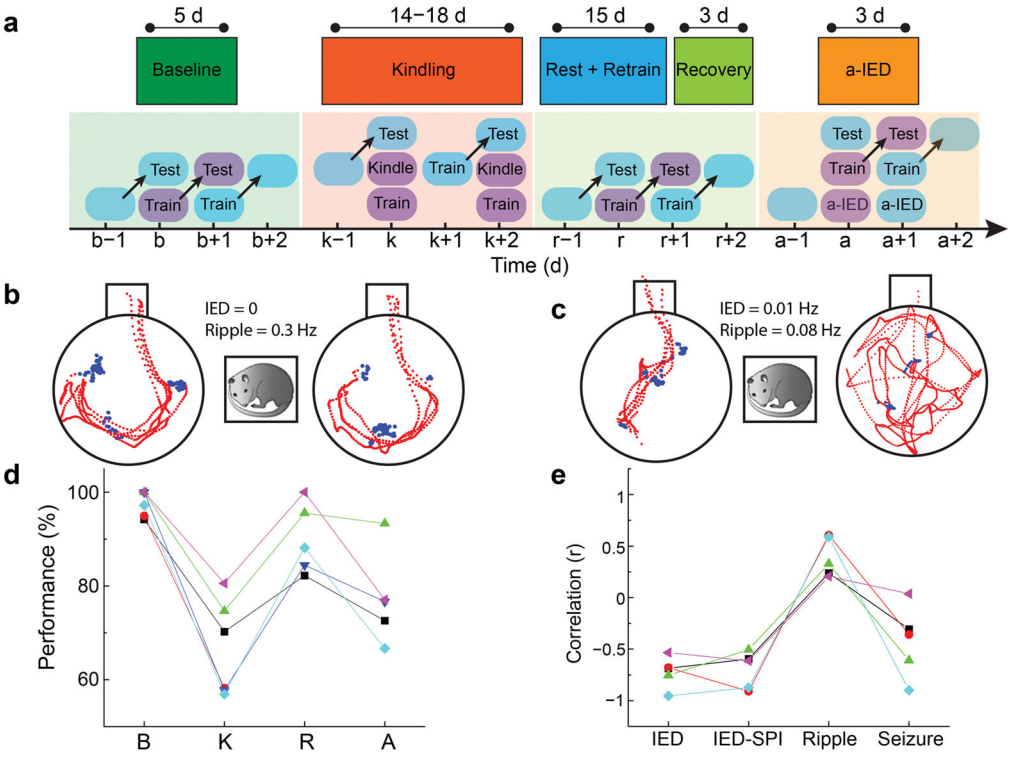

Figure 2.

Hippocampal IEDs impair memory. (**a**) Schematic of behavioral protocol (b = baseline, k = kindling, r = recovery; a = artificial IED). (**b**) Sample baseline behavioral performance. Five overlaid rat trajectories (red) and consummatory periods (blue) for the last five trials of a training session on the cheeseboard maze (left) and the five trials of the corresponding test session 24 h later (right). (**c**) Sample behavioral performance at the end of kindling; conventions as in (**b**). (**d**) Memory performance score on test sessions across the behavioral protocol. Different colors represent scores of individual rats ($n = 6$ for baseline, kindle; $n = 5$ for recovery, a-IEDs). One rat was unable to complete the recovery and a-IEDs phases due to breakage of the hippocampal probe (Kruskal-Wallis ANOVA $P = 3.6 \times 10^{-10}$; Bonferroni correction; baseline/recovery vs. kindle $P = 3.7 \times 10^{-10}$; baseline/recovery vs. a-IED $P = 9.8 \times 10^{-4}$; kindle vs. a-IED $P = 0.4$). (**e**) Multivariate correlation of IED rate, IED-spindle coupling rate, ripple rate, (all in events/s) and cumulative number of seizures with memory performance score. Different colors represent correlations for individual rats ($n = 5$; one animal was eliminated from this statistical analysis due to inability to detect ripples throughout behavioral phases).

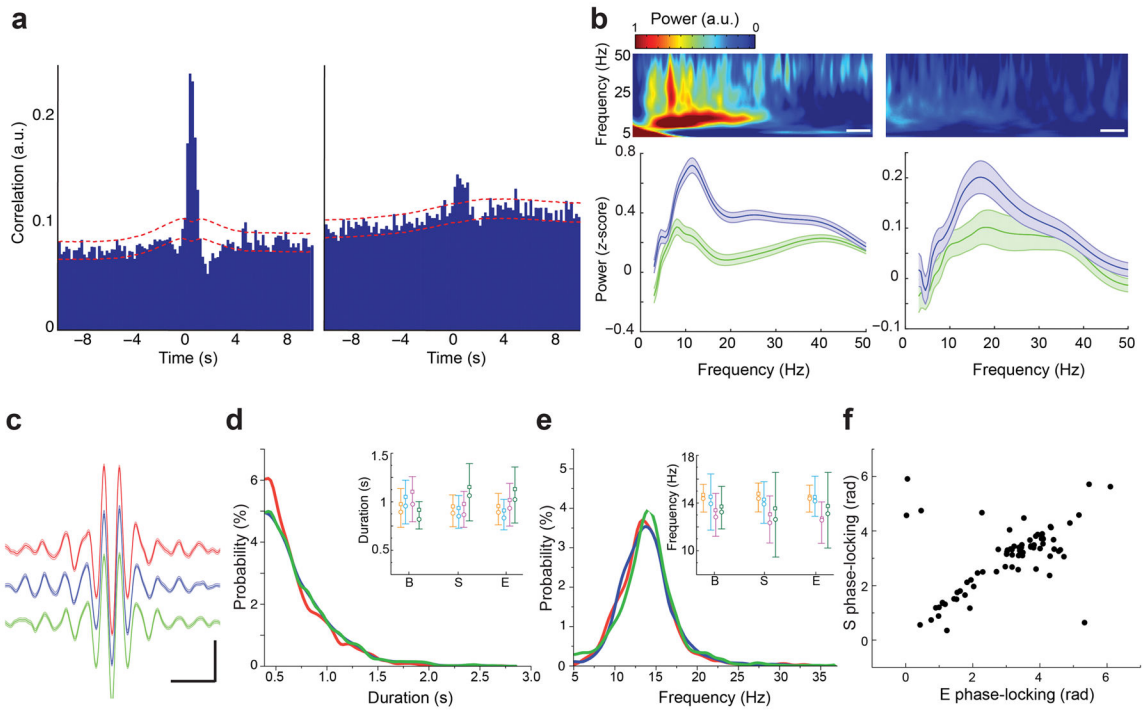

Figure 3.

Correlation of hippocampal IEDs and ripples with mPFC spindles. (**a**) Cross-correlation of IEDs and spindles (left; $n = 47$ sessions from four rats; 15,441 IEDs, 37,835 spindles). Cross-correlation of ripples and spindles (right; $n = 11$ sessions from four rats; 19,109 ripples, 5,919 spindles; red lines = 95% confidence intervals). (**b**) Averaged mPFC spectrogram following hippocampal IED (top left) or ripple (top right; same power scale; scale bar = 200 ms). Averaged power spectrum (bottom; mean ± s.e.m.) before (blue) and after (green) IED or ripple. (**c**) Average filtered spindle waveform in unkindled rats (baseline, B, blue), spontaneous spindle in kindled rats (spontaneous, S, red), and IED-evoked spindle in kindled rats (evoked, E, green; scale bar = 100 μV, 200 ms; $n = 500$ spindles for each group from four rats). (**d**) Probability distribution of duration across spindle types. Inset: changes in mean (open circle) and median (open square) spindle duration in each rat (separate color) across spindle type (box plot tails = 25th and 75th percentiles; Kruskal-Wallis $P = 1.0 \times 10^{-7}$; B vs. S $P = 6.4 \times 10^{-8}$; S vs. E $P = 0.002$ (Bonferroni correction); $n = 1,074$ baseline spindles, 1,236 spontaneous spindles, 1,071 evoked spindles from four rats). (**e**) Probability distribution of frequency for spindle type with changes for each rat (inset). Conventions and n are as in (**d**); $P = 0.04$; S vs. E $P = 0.04$. (**f**) Scatterplot of significantly phase-locked putative mPFC single units to IED-evoked spindles (E) vs. spontaneous spindles (S; Spearman's rho = 0.52; P (Fisher R to Z) = 3×10^{-6}; $n = 74$ units from four rats).

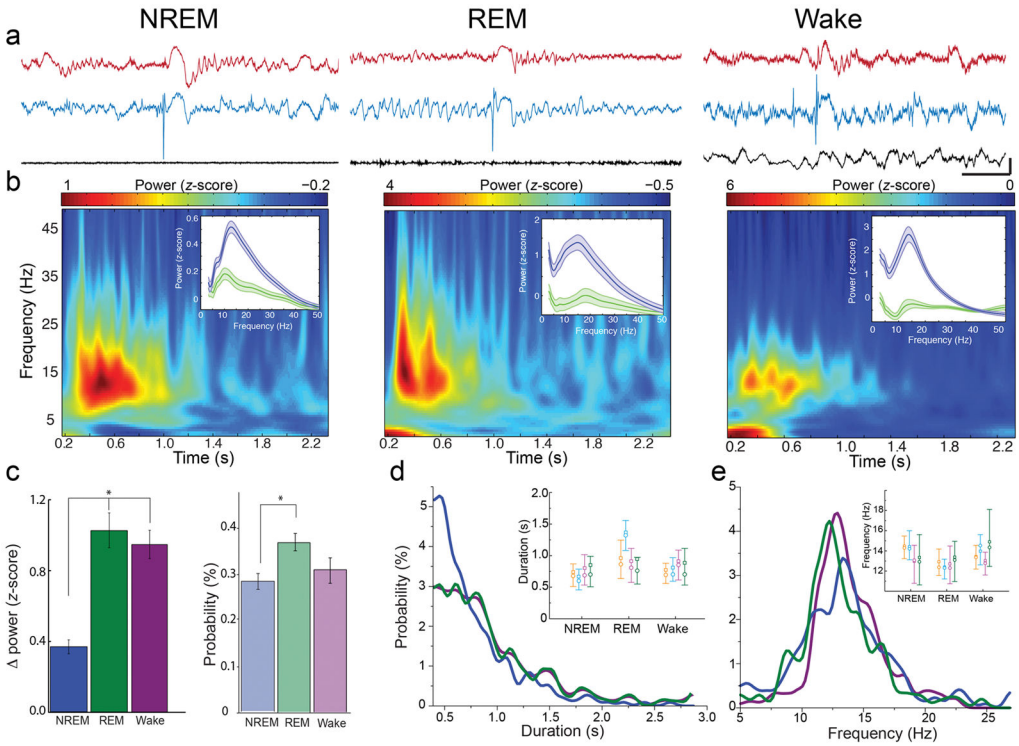

Figure 4.

Hippocampal IEDs trigger mPFC spindles in all behavioral states. (**a**) mPFC (red) and hippocampal (blue) LFP with accelerometer trace (black) demonstrating an IED-evoked spindle in each behavioral state (scale bar = 500 μV, 1 s; traces from two rats). (**b**) Average normalized spectrogram in mPFC following hippocampal IED. Averaged mPFC power spectrum before (blue) and after (green) IED (inset; mean ± s.e.m.). (**c**) Change in mPFC *z*-scored spindle power before vs. after hippocampal IED (dark colored bars; Kruskal-Wallis $P = 7.2 \times 10^{-7}$; NREM vs. REM $P = 4.3 \times 10^{-5}$; NREM vs. Wake $P = 6.1 \times 10^{-6}$; (Bonferroni correction); $n = 17$ NREM, 14 REM, and 14 Wake sessions from four rats). Probability of mPFC spindle following hippocampal IED across states (light colored bars; Kruskal-Wallis $P = 0.04$; NREM vs. REM $P = 0.03$; (Bonferroni correction); $n = 67$ NREM, 98 REM, and 53 Wake sessions from four rats; * = $P < 0.05$). (**d**) Probability distribution of IED-evoked spindle duration in NREM (blue), REM (green), Wake (magenta). Changes in mean (open circle) and median (open square) spindle duration in each rat (inset; separate colors) across states (box plot tails = 25th and 75th percentiles; Kruskal-Wallis $P = 2.0 \times 10^{-4}$; NREM vs. REM $P = 1.1 \times 10^{-4}$; (Bonferroni correction); $n = 220$ NREM spindles, 193 REM spindles, 207 Wake spindles from four rats). (**e**) Probability distribution of IED-evoked spindle frequency in each behavioral state (Conventions and n are as in (**d**); $P = 0.01$; REM vs. Wake $P = 0.01$).

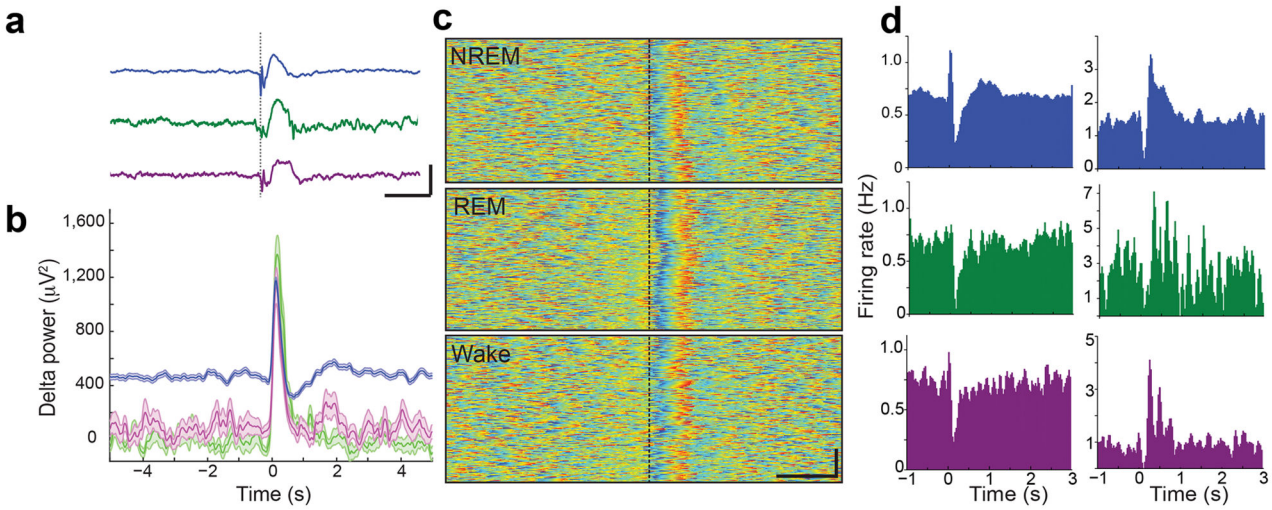

Figure 5.

Hippocampal IEDs trigger cortical 'DOWN' states in the mPFC. (**a**) Averaged raw mPFC LFP in time window bordering hippocampal IED (dashed line) in each behavioral state (blue = NREM, green = REM, magenta = Wake; scale bar = 400 μV, 1 s; *n* = 40 traces from each state in one rat; similar findings in all other rats). (**b**) Average mPFC delta power (mean ± s.e.m.) in each behavioral state (time window, colors, *n* as in (**a**)). Delta power in REM prior to IED was used as adjusted baseline. (**c**) Stacked mPFC delta phases (2–5 Hz) in time window bordering individual hippocampal IEDs (rows) across states (blue = –pi, red = pi; scale bar = 50 trials, 500 ms; *n* = 259 NREM, 268 REM, 236 Wake IED trials from one rat; similar findings in all other rats). (**d**) Average peri-event firing rate histograms of representative putative mPFC pyramidal cells (left) and interneurons (right) in the time window bordering hippocampal IED (time zero; colors as in (**a**); *n* = 405 pyramidal cells and 22 interneurons from sample rat).

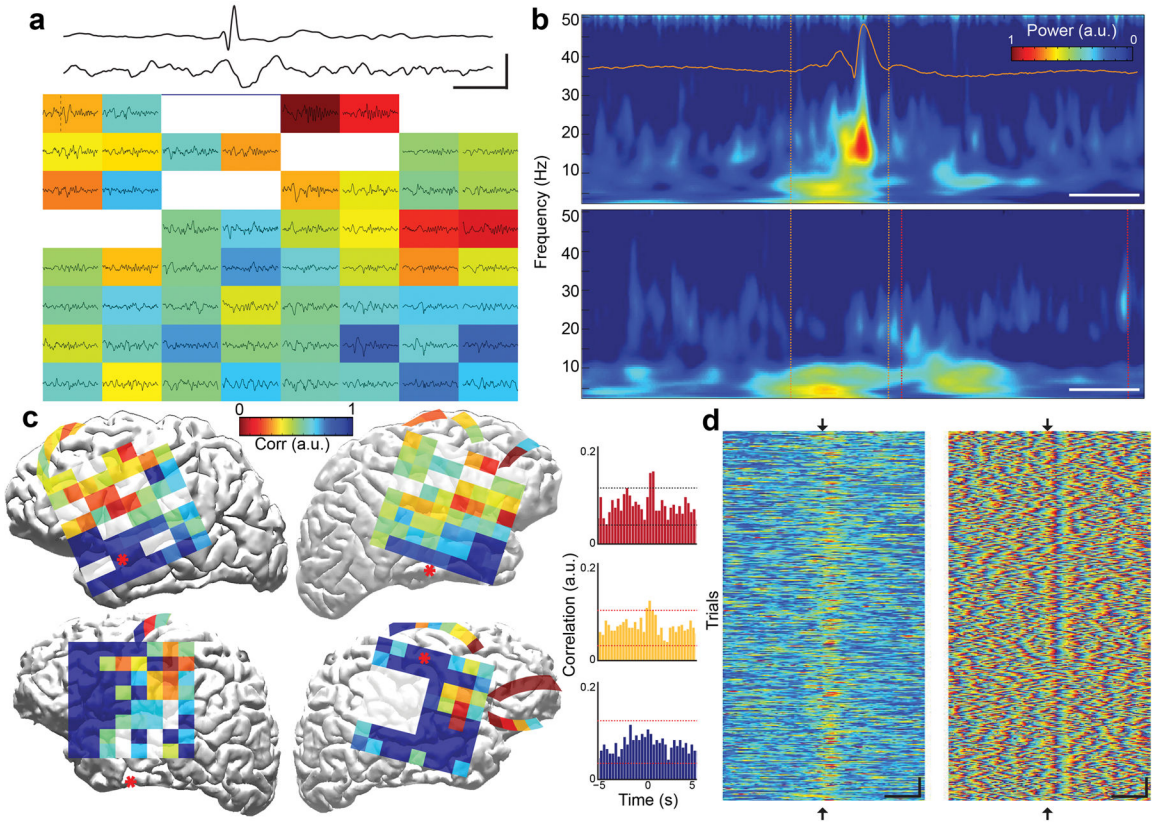

Figure 6.

IEDs in subjects with epilepsy trigger cortical spindles. (**a**) LFP from IED electrode (upper; depth electrode in parahippocampal gyrus) demonstrating typical IED and subdural cortical electrode (lower; grid electrode in frontal cortex) demonstrating time-locked spindle. Grid shows *z*-scored spindle band power across cortical ECoG array triggered on above IED (occurrence time indicated by dashed line). White channels are nonfunctional (scale bar = 100 μV, 200 ms; duration of each grid LFP trace = 1.6 s). (**b**) Average spectrograms triggered on IED occurrence (orange box) for IED electrode (upper panel; sample IED LFP in orange), and a representative cortical grid electrode (lower panel; red box = time of spindle; scale bar = 1 s; n = 798 IED trials from one subject; similar results for all other subjects). (**c**) Schematic of ECoG grid and strip placement (each square = one recording electrode) on the projected pial surface of four subjects with epilepsy (high IED-spindle correlation = warm colors; low correlation = cool colors; Corr = normalized correlation). Cross-correlograms for high, intermediate, and low correlation electrodes from a sample subject on the right (three sessions for each of four subjects; total of 3,969, 2,077, 1,035, and 1,240 IEDs). Red '*' shows location of IED electrode. (**d**) Stacked trials of delta power (left) and delta phase (right) in a cortical electrode centered on IED occurrence (blue = –pi, red = pi; scale bar = 25 trials, 500 ms; arrowhead = time of IED; n = 477 IED trials from one subject; similar results for all other subjects).